Figure 1

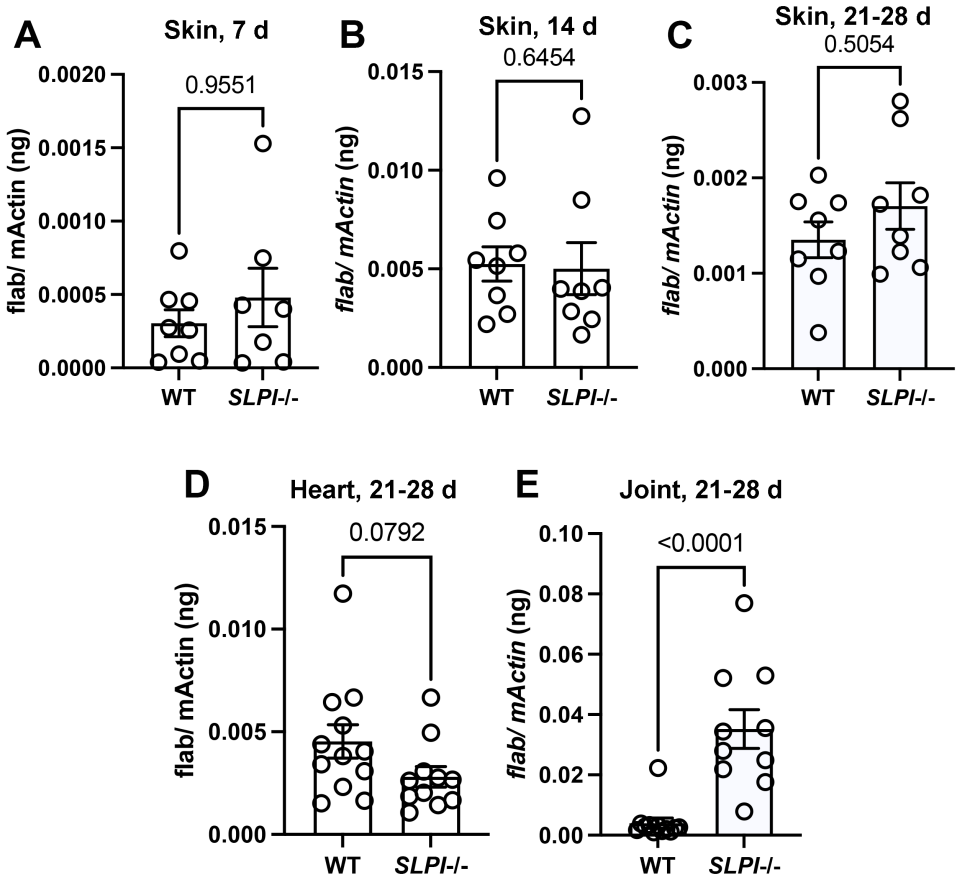
A
Skin, 7 d
0.9551
flab/ mActin (ng)
0.0020
0.0015
0.0010
0.0005
0.0000
WT
SLPI-/-
B
Skin, 14 d
0.6454
flab/ mActin (ng)
0.015
0.010
0.005
0.000
WT
SLPI-/-
C
Skin, 21-28 d
0.5054
flab/ mActin (ng)
0.003
0.002
0.001
0.000
WT
SLPI-/-
D
Heart, 21-28 d
0.0792
flab/ mActin (ng)
0.015
0.010
0.005
0.000
WT
SLPI-/-
E
Joint, 21-28 d
<0.0001
flab/ mActin (ng)
0.10
0.08
0.06
0.04
0.02
0.00
WT
SLPI-/-

Figure 2

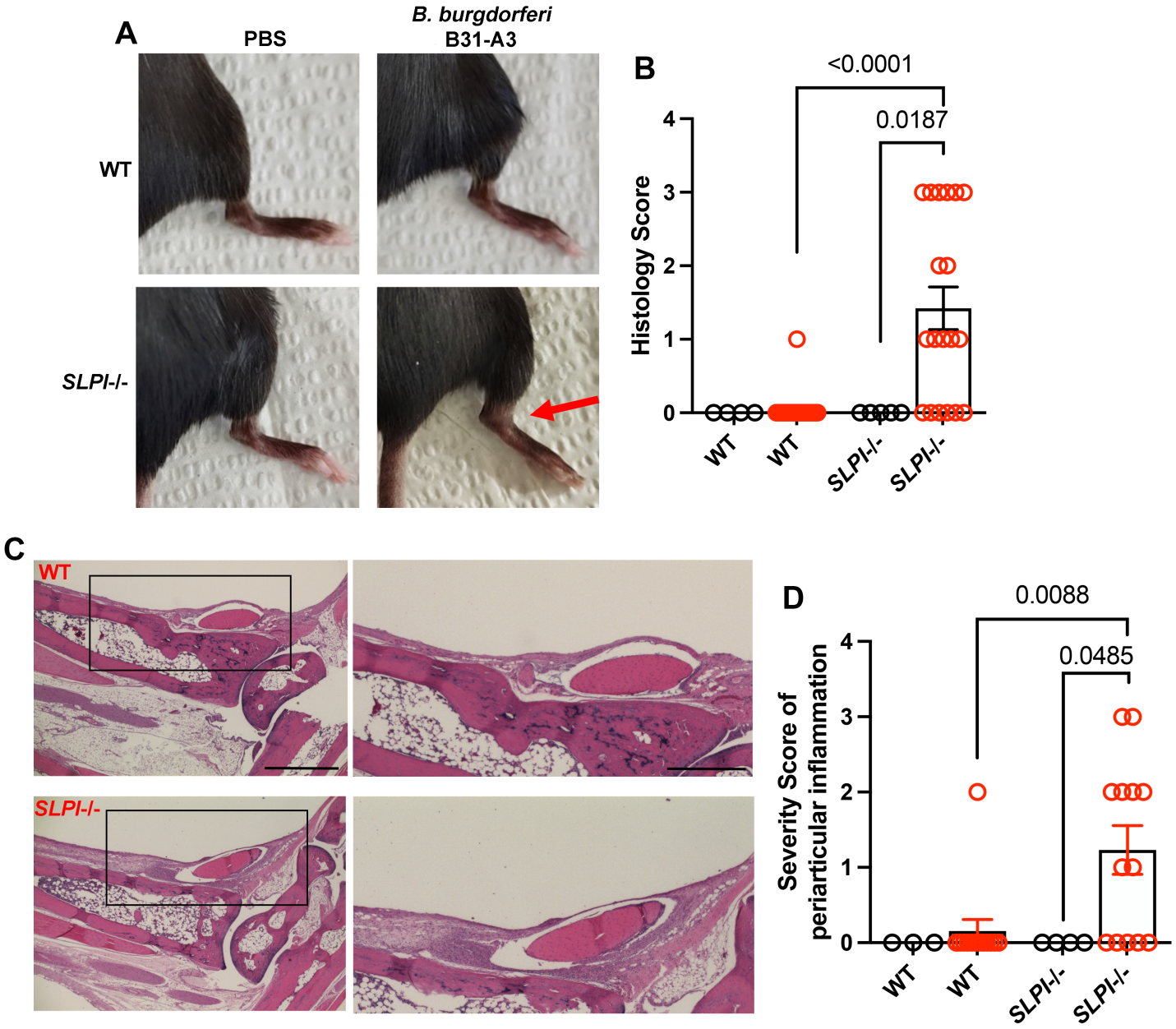
A
PBS
B. burgdorferi
B31-A3
WT
SLPI-/-
B
<0.0001
0.0187
Histology Score
4
3
2
1
0
WT
WT
SLPI-/-
SLPI-/-
C
WT
SLPI-/-
D
0.0088
0.0485
Severity Score of periarticular inflammation
4
3
2
1
0
WT
WT
SLPI-/-
SLPI-/-

Figure 3

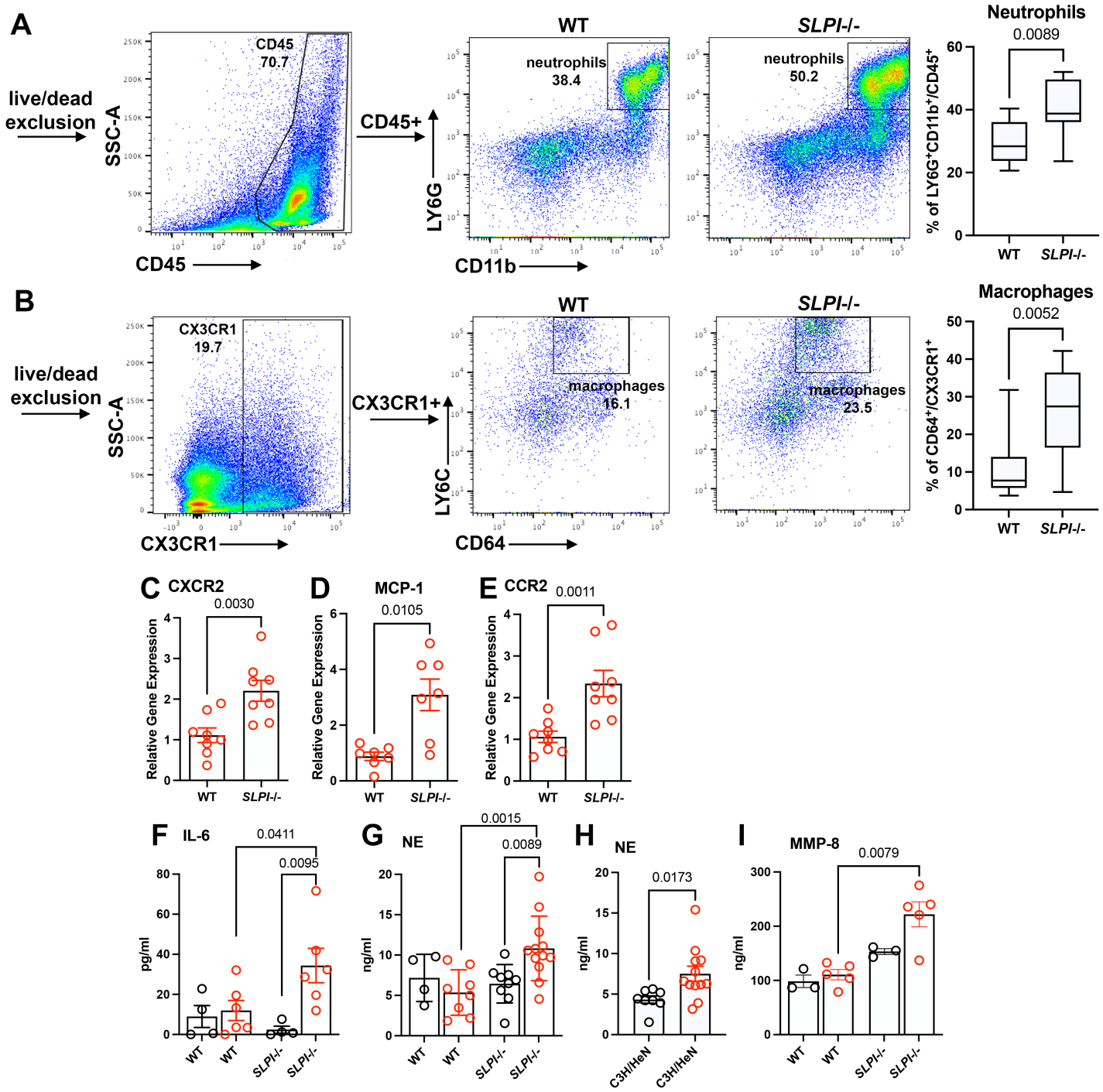
A
live/dead exclusion
SSC-A
CD45
CD45 70.7
CD45+
LY6G
CD11b
WT
SLPI-/-
neutrophils 38.4
neutrophils 50.2
Neutrophils
0.0089
% of LY6G+CD11b+/CD45+
B
live/dead exclusion
CX3CR1
CX3CR1 19.7
CX3CR1+
LY6C
CD64
macrophages 16.1
macrophages 23.5
Macrophages
0.0052
% of CD64+/CX3CR1+
C CXCR2
0.0030
D MCP-1
0.0105
E CCR2
0.0011
Relative Gene Expression
F IL-6
0.0411
0.0095
pg/ml
G NE
0.0015
0.0089
ng/ml
H NE
0.0173
C3H/HeN
I MMP-8
0.0079

Figure 4

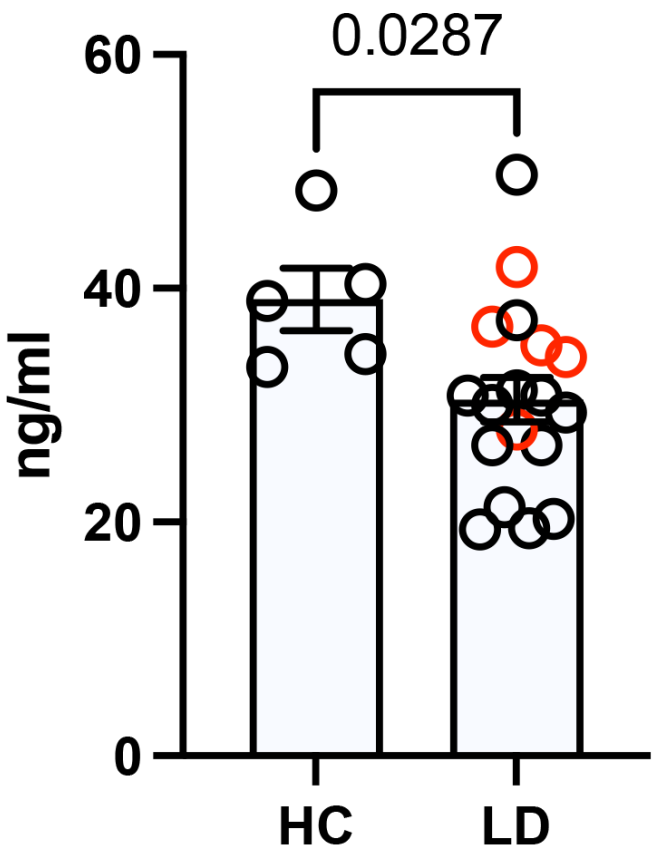

Figure 5

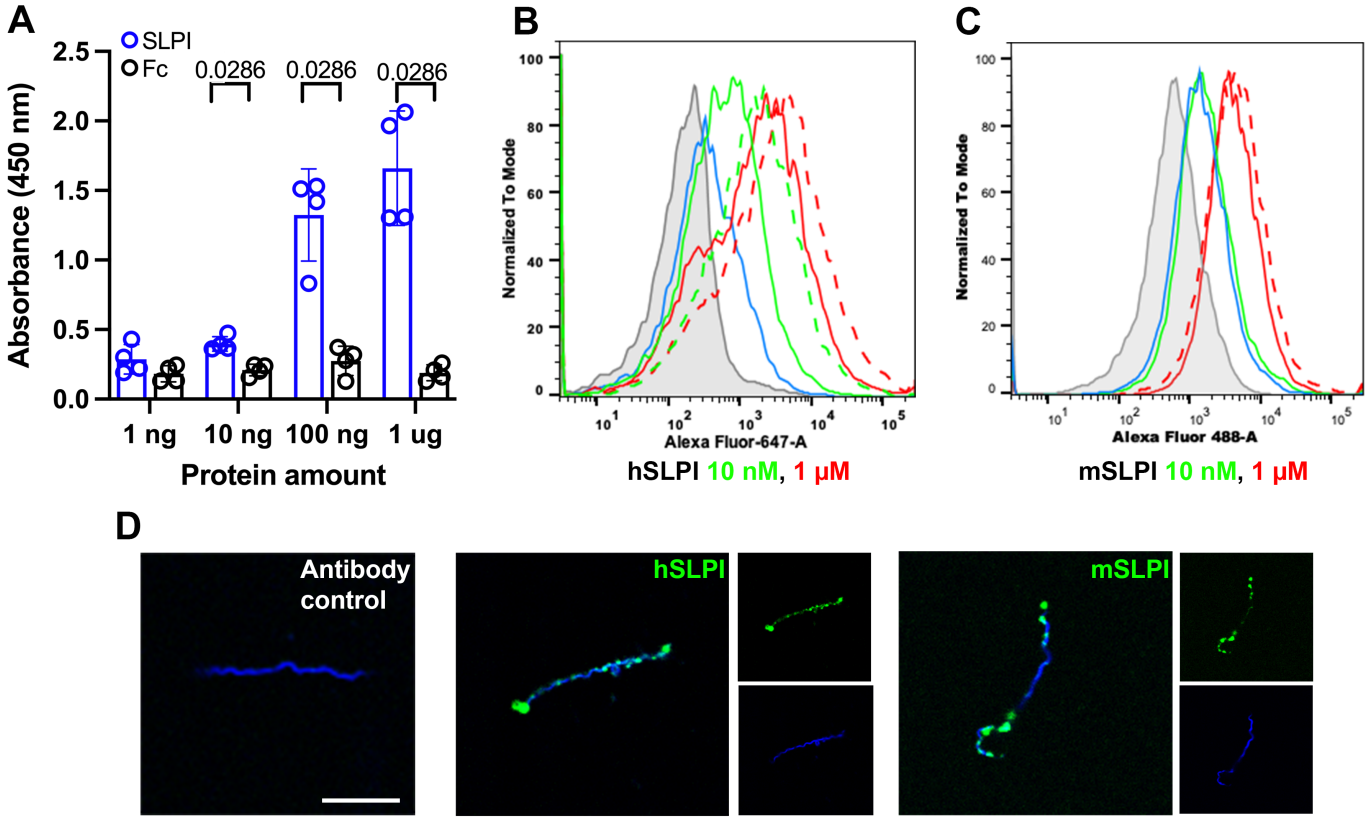
A
SLPI
Fc
0.0286
0.0286
0.0286
Absorbance (450 nm)
2.5
2.0
1.5
1.0
0.5
0.0
1 ng
10 ng
100 ng
1 ug
Protein amount
B
Normalized To Mode
Alexa Fluor-647-A
hSLPI 10 nM, 1 μM
C
Normalized To Mode
Alexa Fluor 488-A
mSLPI 10 nM, 1 μM
D
Antibody control
hSLPI
mSLPI

Secretory leukocyte protease inhibitor influences periarticular joint inflammation in *B. burgdorferi*-infected mice

Qian Yu[1*], Xiaotian Tang[1,7], Thomas Hart[1], Robert Homer[2], Alexia A. Belperron[3], Linda K. Bockenstedt[3], Aaron Ring[4,5], Akira Nakamura[6], Erol Fikrig[1]

[1]Section of Infectious Diseases, Department of Internal Medicine, School of Medicine, Yale University, New Haven, Connecticut, USA. [2]Department of Pathology, School of Medicine, Yale University, New Haven, Connecticut, USA. [3] Section of Rheumatology, Allergy and Immunology, Department of Internal Medicine, School of Medicine, Yale University, New Haven, Connecticut, USA. [4]Department of Immunobiology, Yale School of Medicine, New Haven, CT, USA. [5]Department of Pharmacology, Yale School of Medicine, New Haven, CT, USA. [6]Divisions of Immunology, Faculty of Medicine, Tohoku Medical and Pharmaceutical University, Sendai, Japan.[7]Institute of Insect Sciences, College of Agriculture and Biotechnology, Zhejiang University, Hangzhou, China.

Corresponding authors:

Qian Yu, The Anlyan Center, 300 Cedar St. Rm 410, New Haven, CT, 06519, USA, (203)-843-8578, qian.yu@yale.edu

Authorship note: Qian Yu and Xiaotian Tang are co–first authors.

Conflict-of-interest: The authors have no conflicts of interest.

Abstract

Lyme disease, caused by *Borrelia burgdorferi*, is the most common tick-borne infection in the United States. Arthritis is a major clinical manifestation of infection, and synovial tissue damage has been attributed to the excessive pro-inflammatory responses. The secretory leukocyte protease inhibitor (SLPI) promotes tissue repair and exerts anti-inflammatory effects. The role of SLPI in the development of Lyme arthritis in C57BL/6 mice, which can be infected with *B. burgdorferi*, but only develop mild joint inflammation, was therefore examined. *SLPI*-deficient C57BL/6 mice challenged with *B. burgdorferi* had a higher infection load in the tibiotarsal joints and marked periarticular swelling, compared to infected wild type control mice. The ankle joint tissues of *B. burgdorferi*-infected *SLPI*-deficient mice contained significantly higher percentages of infiltrating neutrophils and macrophages. *B. burgdorferi*-infected *SLPI*-deficient mice also exhibited elevated serum levels of IL-6, neutrophil elastase, and MMP-8. Moreover, using a recently developed BASEHIT (**BA**cterial **S**election to **E**lucidate **H**ost-microbe **I**nteractions in high **T**hroughput) library, we found that SLPI directly interacts with *B. burgdorferi*. These data demonstrate the importance of SLPI in suppressing periarticular joint inflammation in Lyme disease.

43 **Introduction**

44

45 Lyme disease is the most common tick-borne illness in the United States,
46 affecting an estimated 500,000 people each year[1]. The spirochete *Borrelia burgdorferi* is
47 the causative agent of Lyme disease and is primarily transmitted by *Ixodes scapularis*
48 ticks in North America[2]. Early administration of antibiotics is usually successful in the
49 treatment of Lyme disease. However, between 2008-2015, arthritis was the major
50 manifestation in a third of Lyme disease cases reported to CDC[3,4]. Musculoskeletal
51 symptoms occur at all stages of Lyme disease, with migratory arthralgias in the early
52 stages and frank arthritis occurring months later. Lyme arthritis can present as acute or
53 intermittent self-resolving episodes or persistent joint swelling and pain, which if left
54 untreated, can lead to irreversible joint dysfunction and debilitation[3,5,6]. Although Lyme
55 arthritis resolves completely with antibiotic therapy in most patients, a small percentage
56 of individuals experience persistent joint inflammation for months or several years,
57 termed post-infectious Lyme arthritis[3,5,7].

58

59 Studies of synovial fluid from Lyme arthritis patients found infiltrating
60 polymorphonuclear cells (PMNs), IFN-γ-producing mononuclear cells, and large
61 amounts of NF-κB-induced pro-inflammatory cytokines and chemokines, such as IL-6,
62 CXCL10, and TNF-α[6,8-10]. An inverse correlation between the robust IFN-γ signature
63 and tissue repair has been demonstrated in the synovial tissue and fluid from patients
64 with post-infectious Lyme arthritis[11]. This suggests that the dysregulated excessive pro-
65 inflammatory responses inhibit tissue repair and lead to extensive tissue damage.

66

67 *B. burgdorferi* infection of laboratory mice causes an acute arthritis, the severity
68 of which is mouse strain dependent[12]. *B. burgdorferi* infected-C3H/HeN mice develop
69 pronounced neutrophilic infiltration of periarticular structures and the synovial lining
70 which peaks in severity several weeks after infection[13]. In contrast, infection of *B.*
71 *burgdorferi* C57BL/6 mice causes mild, if any, arthritis[14]. On a C57BL/6 background, the
72 immune-deficient RAG-/- and SCID mice are also resistant to *B. burgdorferi*-induced
73 arthritis, indicating that responses independent of humoral and cellular immunity
74 contribute to the milder phenotype of disease in these animals[15]. Similar to Lyme
75 arthritis in humans, neutrophils, macrophages, and signaling involving IFN-γ and NF-κB
76 contribute to the severity of murine joint inflammation[16-19].

77

78 The secretory leukocyte protease inhibitor (SLPI) is a 12 kDa, secreted, non-
79 glycosylated, cysteine-rich protein[20]. It strongly inhibits serine proteases, especially
80 neutrophil-derived serine proteases (NSPs) including cathepsin G (CTSG) and elastase
81 (NE)[21,22]. It is secreted by epithelial cells at various mucosal surfaces and is also
82 produced by neutrophils, macrophages, mast cells, and fibroblasts[23,24]. The major
83 function of SLPI is to inhibit excessive protease activity at sites of inflammation, thus
84 promoting tissue repair and wound healing[25,26]. SLPI also exerts anti-inflammatory
85 function by inhibiting NF-κB activation in macrophages[27-29]. The roles of neutrophils and
86 NSPs have been extensively studied in rheumatoid arthritis, a condition sharing some
87 similarities with Lyme arthritis[30,31]. NE and CTSG induce potent destruction of cartilage
88 proteoglycan *in vitro* and *in vivo*, which contributes to rheumatoid arthritis progression[32].

89 Some studies also demonstrated that SLPI inhibits joint inflammation and bone
90 destruction[33,34]. However, the importance of SLPI and NSPs have not been studied in
91 the context of Lyme disease. Thus, in this study, we examined the role of SLPI in the
92 development of murine Lyme arthritis caused by *B. burgdorferi*.
93

Results

Secretory leukocyte protease inhibitor (SLPI) influences periarticular joint inflammation in B. burgdorferi-infected mice.

To assess the importance of SLPI during murine Lyme arthritis, we compared the outcomes of *B. burgdorfe*ri infection of C57BL/6 WT and *SLPI*-/- mice. The C57BL/6 WT and *SLPI*-/- mice were infected with 10^5 spirochetes subcutaneously. Infection burdens in the skin were assessed by qPCR of *B. burgdorferi* DNA in ear punch biopsies at 7, 14, and 21 to 28 dpi (Figure 1, A-C). Infection burdens in the heart (Figure 1D) and tibiotarsal joint (Figure 1E) tissues were assessed at 21 to 28 dpi. We did not observe any significant difference in infection burden in the skin between WT and *SLPI*-/- mice (n=24) at 7, 14, 21 to 28 dpi, or in the heart at 21 to 28 dpi (Figure 1, A-D).

Strikingly, we observed a significantly higher spirochete burden in the ankle joints of infected *SLPI*-/- mice (n=24) at 21 to 28 dpi (Figure 1E). Furthermore, at around 28 dpi, significant swelling was also observed solely in the infected *SLPI*-/- mice (Figure 2A, red arrow). The level of swelling was first scored visually. While 14 out of 20 infected *SLPI*-/- mice displayed visible swelling (score ≥ 1), only 1 in 14 infected WT mice displayed mild swelling (score 1) at the ankle (Figure 2B). The tibiotarsal joints were then dissected, fixed, and stained with H&E for histopathological evaluation of the level of inflammation (Figure 2, C and D). Inflammation of bursa and soft tissue adjacent to the tibiotarsal joint, but not in the tibiotarsal synovium, was consistently observed in the

117 infected *SLPI*-/- mice (Figure 2C, black rectangle). In contrast, only 1 out of 14 infected
118 WT mice displayed modest inflammation (score = 2) in these sites (Figure 2D). The
119 above data indicate the importance of SLPI in modulating the development of
120 periarticular inflammation associated with murine Lyme arthritis.
121
122 ***SLPI influences immune responses in B. burgdorferi-infected mice.***
123
124 It has been established that SLPI exerts its anti-inflammatory effect by inhibiting
125 neutrophil serine protease and by dampening NF-κB activation in macrophages[22]. Thus,
126 to investigate the mechanism underlying the effect of SLPI on murine joint inflammation,
127 we sought to identify the population of infiltrating cells in the periarticular tissues of
128 infected WT and *SLPI*-/- mice. At 21-28 dpi, the ankle joints were dissected. To obtain
129 single cell suspensions of infiltrating cells, bone marrow cells were removed and
130 discarded and the joint and periarticular tissues were digested[35]. The cells were stained
131 for flow cytometry with CD45, CD11b, and LY6G to label neutrophils (Figure 3A), and
132 CX3CR1, CD64, and LY6C to label macrophages (Figure 3B)[36]. After gating, we
133 observed significantly higher percentages of infiltrating neutrophils and macrophages in
134 the dissected tissues from infected *SLPI*-/- than WT mice (Figure 3, A and B). Using RT-
135 qPCR on the tibiotarsal tissues extracted from *B. burgdorferi*-infected *SLPI*-/- mice, we
136 detected increased gene expression of neutrophil chemoattractant receptor *CXCR2*,
137 monocyte chemoattractant protein 1 (*MCP-1*), and its receptor *CCR2* (Figure 3, C-E).
138

139 Furthermore, the serum cytokine/chemokine profile was assessed from
140 uninfected and *B. burgdorferi*-infected WT and *SLPI*-/- mice at 28 dpi. We observed a
141 significant increase in IL-6 in infected *SLPI*-/- mice (Figure 3F). IL-6 recruits and
142 stimulates neutrophils, leading to secretion of neutrophil-derived serine proteases
143 including neutrophil elastase (NE) and cathepsin G (CTSG)[37]. The lack of serine
144 protease inhibitors, such as SLPI, can cause excessive protease activity and
145 subsequent tissue damage and inflammation[31]. Indeed, using ELISA, we observed a
146 significantly higher level of NE solely in the serum of infected *SLPI*-/- mice (Figure 3G).
147 An increased serum level of NE was also observed in the *B. burgdorferi*-infected,
148 arthritis-susceptible C3H/HeN mice at 21 dpi (Figure 3H). These data suggest that, in
149 the absence of SLPI, excessive serine protease activity can exacerbate murine Lyme
150 arthritis.
151
152 A correlation between IL-6, macrophages, metalloproteinases (MMPs), and
153 articular cartilage destruction has been observed in the synovial tissue of RA patients[38].
154 Elevated levels of host matrix metalloproteinases (MMPs) have also been found in the
155 synovial fluid of Lyme arthritis patients and can cause excessive tissue damage[39]. Thus,
156 a mouse MMP 5-Plex Discovery Assay was used to explore the serum levels of different
157 MMPs. We observed a significant increase in the levels of MMP-8 solely in the infected
158 *SLPI*-/- mice (Figure 3I). Taken together, our data suggest that SLPI suppresses
159 inflammation in *B. burgdorferi*-infected mouse joint tissues by potentially inhibiting
160 neutrophil and macrophage infiltration and subsequent protease-mediated tissue
161 destruction.

162

163 ***Decreased serum level of SLPI in Lyme disease patients*.**

164

165 Despite numerous studies of serum, synovial fluid and tissue from Lyme arthritis
166 patients, the importance of anti-protease-protease balance in Lyme arthritis has not
167 been investigated[7]. Based on our data obtained from the *SLPI*-deficient mice, we
168 assessed the serum SLPI level in Lyme disease patients (Figure 4). Due to the limited
169 samples available from Lyme arthritis patients, we included samples from Lyme disease
170 patients who presented with earlier manifestations of Lyme disease. The serum level of
171 human SLPI assessed by ELISA showed a significant decrease in the SLPI level in
172 Lyme disease patients comparing to healthy adult controls (Figure 4). Similar to our data
173 from *B. burgdorferi*-infected mice, this result suggests a correlation between the lack of
174 SLPI and humans exhibiting clinical manifestations of Lyme disease, including arthritis.

175

176 ***SLPI interacts with B. burgdorferi.***

177

178 It has been demonstrated that *B. burgdorferi* interacts with various mammalian
179 proteins to establish infection in the mammalian host[40-43]. Thus, we postulated that *B.*
180 *burgdorferi* could interact with SLPI to influence the progression of joint inflammation. To
181 test this hypothesis, we probed a recently developed BASEHIT (**BA**cterial **S**election to
182 **E**lucidate **H**ost-microbe **I**nteractions in high **T**hroughput) library with *B. burgdorferi*[40,44-
183 46]. Human SLPI is one of the exoproteins that passed the significance threshold,
184 indicating *B. burgdorferi*-SLPI binding. To further establish that hSLPI directly binds to *B.*

185 *burgdorferi*, we performed ELISA with whole cell *B. burgdorferi* lysates. We observed
186 strong binding between whole cell *B. burgdorferi* lysates and hSLPI at a level as low as
187 10 nM (Figure 5A).
188
189 To extend these studies, flow cytometry was performed using intact *B.*
190 *burgdorferi* and both human and murine SLPI. A significant increase in fluorescence
191 intensity was observed when *B. burgdorferi*, cultivated at 33°C, was incubated with
192 human SLPI at 10 nM and 1 μM level (Figure 5B). Though the binding to 10 nM rmSLPI
193 was at background level, we observed a significant increase in fluorescence intensity
194 when *B. burgdorferi* were incubated with 1 μM rmSLPI (Figure 5C). Flow cytometry also
195 demonstrated increased binding of *B. burgdorferi* cultured at 37 °C to 1 μM hSLPI or
196 rmSLPI (Figure 5, B and C). This indicates that the binding was more robust when
197 performed at temperatures that *B. burgdorferi* encounter in the mammalian host.
198 Immuno-fluorescent microscopy was an additional method that also demonstrated direct
199 binding of *B. burgdorferi* with human or murine SLPI (Figure 5D).
200
201 In contrast to *B. burgdorferi* B31-A3, an infectious strain used throughout this
202 study, we did not observe any binding between hSLPI and *B. burgdorferi* B31A, a high-
203 passage non-infectious strain (Supplemental Figure 1A)[47,48]. The above observation
204 further suggests that the direct interaction between SLPI and *B. burgdorferi* could
205 impact the pathogenesis of murine Lyme arthritis. To further investigate the potential *B.*
206 *burgdorferi* ligand that interacts with SLPI, we probed protease-treated *B. burgdorferi*
207 lysates with hSLPI using ELISA. After treatment with proteinase K, we observed a

208 marked decrease in binding of hSLPI to *B. burgdorferi* lysates (Supplemental Figure
209 1B). This result suggests that hSLPI can directly interact with a *B. burgdorferi* protein.
210
211 It has been showed that SLPI has antimicrobial effects against multiple gram-
212 negative and positive bacteria[49-51]. However, using the BacTiter-Glow microbial cell
213 viability assay, we did not observe any significant changes in *B. burgdorferi* viability in
214 the presence of hSLPI (Supplemental Figure 2A). A previous study also demonstrated
215 that the tick salivary protein, Salp15, specifically interacted with *B. burgdorferi* outer
216 surface protein C (OspC)[52]. The binding of Salp15 protected spirochetes from killing by
217 polyclonal mouse or rabbit antisera *in vitro*[52,53]. However, again, using the BacTiter-
218 Glow microbial cell viability assay, the pre-incubation of hSLPI did not protect
219 spirochetes from killing by mouse *B. burgdorferi* antisera (Supplemental Figure 2B).
220 Thus, the importance of the SLPI-*B. burgdorferi* interaction and the direct effect of such
221 an interaction on *B. burgdorferi* biology is likely independent of direct borreliacidal
222 activity or any interference with the antibody-mediated *B. burgdorferi* killing.
223

224 **Discussion**

225

226 Lyme arthritis has been extensively documented and studied in patients and *B.*
227 *burgdorferi*-infected mice. The pathogenesis of Lyme arthritis is characterized by
228 synovial tissue damage caused by infiltration of immune cells and excessive pro-
229 inflammatory responses[7]. Transcriptomic studies also revealed the suppression of
230 tissue repair genes in the synovial tissue of Lyme arthritis patients and tibiotarsal joint
231 tissues of *B. burgdorferi*-infected mice[11,54]. However, the roles of the genes involved in
232 tissue repair have not been studied.

233

234 SLPI strongly inhibits serine proteases, especially cathepsin G and elastase
235 secreted by neutrophils[20]. The major function of SLPI is to prevent unnecessary tissue
236 damage caused by excessive protease activity, thus promoting tissue repair and
237 homeostasis[55]. The lack of SLPI impairs wound healing and tissue repair [25] and SLPI
238 also inhibits NF-κB activation and downstream pro-inflammatory cytokine release from
239 macrophages[27,29]. Thus, we hypothesized that SLPI plays an important role in Lyme
240 arthritis. To test this hypothesis, we employed *SLPI*-/- C57BL/6 mice. As C57BL/6 mice
241 only develop mild arthritis, if any, after challenge with *B. burgdorferi*, this mouse
242 provided an ideal example to study whether the lack of SLPI could cause an arthritis-
243 resistant mouse to become arthritis-susceptible. Compared to WT C57BL/6 mice, *B.*
244 *burgdorferi* infection in the *SLPI*-/- mice consistently showed a significantly higher
245 infection burden in tissues extracted from the ankle joint, which included periarticular
246 structures (Figure 1E). Severe swelling and inflammation in the bursal and soft tissue

247 around tibiotarsal joints were observed solely in the infected *SLPI*-/- mice (Figure 2).
248 These data emphasize the importance of SLPI in controlling the development of
249 inflammation in periarticular tissues of *B. burgdorferi*-infected mice. Indeed, in a
250 *Streptococcal* cell wall (SCW)-induced arthritis model in rats, the intraperitoneal
251 injection of SLPI significantly decreased the severity of joint swelling[34]. Targeting the
252 SLPI-associated anti-protease pathways could also potentially be a strategy for
253 ameliorating periarticular inflammation that occurs in some rheumatic diseases.
254
255 Analysis of *B. burgdorferi* infection in the *SLPI*-/- and WT mice revealed a
256 significant increase in infiltrating neutrophils and macrophages in the periarticular
257 tissues of *SLPI*-/- mice (Figure 3, A and B). This observation is consistent with clinical
258 studies that showed a high percentage of neutrophils in the synovial fluid during active
259 infection[56,57]. In post-treatment Lyme arthritis, fewer neutrophils and more macrophages
260 are present in patients' synovial fluid[7]. In arthritis-susceptible C3H/He mice, *B.*
261 *burgdorferi* infection also leads to neutrophil infiltration in the periarticular tissues as well
262 as in the synovium of ankle joints[13]. The neutrophil chemoattractant KC (CXCL1) and
263 receptor CXCR2 mediates neutrophil recruitment and is critical for the development of
264 murine Lyme arthritis. Both *KC*-/- and *CXCR2*-/- C3H mice developed significantly less
265 ankle swelling when infected with *B. burgdorferi*[16,18]. Consistently, we observed a
266 significant increase in CXCR2 gene expression in the tibiotarsal joint tissues (Figure
267 3C), which can recruit neutrophils and cause more severe inflammatory soft tissue
268 infiltrates in the *SLPI*-/- mice. Monocyte chemoattractant protein-1 (MCP-1/CCL2) and
269 receptor CCR2 contribute to macrophage infiltration[58]. Though little to no difference in

270 arthritis was observed in the CCR2-/- mice, a high level of MCP-1 was detected in the
271 tibiotarsal tissues of *B. burgdorferi*-infected, arthritis-susceptible C3H/He mice,
272 suggesting a function for macrophages[18]. In the infected *SLPI*-/- mice, a significant
273 increase in both MCP-1 and CCR2 gene expression was observed in the tibiotarsal
274 tissues (Figure 3, D and E). Our data suggest that both neutrophils and macrophages
275 contribute to the severe periarticular inflammation in the infected *B. burgdorferi*-infected
276 *SLPI*-/- mice.
277
278 To investigate the underlying mechanism whereby SLPI deficiency enhanced
279 periarticular joint inflammation, we examined the serum cytokine/chemokine profile of *B.*
280 *burgdorferi*-infected *SLPI*-/- and WT mice. There was a significant increase in IL-6 solely
281 in the infected *SLPI*-/- mice (Figure 3F). An elevated IL-6 level has been demonstrated
282 in the serum, synovial fluid, and synovial tissue from Lyme arthritis patients[9,56]. IL-6 is
283 also pivotal in the pathogenesis of rheumatoid arthritis and correlates with the disease
284 severity and joint destruction[37]. It has been shown that IL-6 recruited neutrophils in an *in*
285 *vitro* co-culture rheumatoid arthritis model[59]. Neutrophils can be activated by IL-6
286 through binding of IL-6 receptor (IL-6R)[37]. Activated neutrophils release several
287 neutrophil serine proteases (NSPs) including neutrophil elastase (NE), cathepsin G
288 (CTSG), and proteinase-3 (PR3), which can lead to potent cartilage destruction[31].
289 Indeed, we observed a significant increase in the NE level in the serum of *B.*
290 *burgdorferi*-infected *SLPI*-/- but not WT mice (Figure 3G). In the arthritis susceptible
291 C3H/HeN mice, *B. burgdorferi* infection also induced a significant increase in the serum
292 NE level (Figure 3H). The above data indicate that the excessive serum neutrophil

293 elastase contributed to the periarticular inflammation in the *B. burgdorferi*-infected *SLPI*-
294 /- mice.
295
296 Matrix metalloproteinases (MMPs) target extracellular matrix and cause articular
297 cartilage destruction[60]. A correlation between IL-6 and MMPs expression has been
298 reported in the context of rheumatoid arthritis[38,61]. Elevated levels of several MMPs
299 have also been found in the synovial fluid of Lyme arthritis patients[39]. Thus, we also
300 investigated the MMPs profile in the *B. burgdorferi*-infected *SLPI*-/- and WT mice. We
301 observed a significant increase in the serum level of MMP-8 in the infected *SLPI*-/- mice
302 (Figure 3I). MMP-8 is known as neutrophil collagenase[62]. Using synovial fluid samples,
303 it has been reported that the level of MMP-8 was significantly higher in the patients with
304 post infectious Lyme arthritis than patients with active infection[63]. A comprehensive
305 examination of the MMP profile in the synovial fluid of patients with Lyme arthritis
306 revealed elevated levels of MMP-1, -3, -13, and -19[64]. *B. burgdorferi* infection induced
307 MMP-3 and MMP-19 in the C3H/HeN mice but not in the Lyme arthritis-resistant
308 C57BL/6 mice[64]. The differences in the MMP profiles provide an explanation for the
309 differences between human and murine Lyme arthritis. This finding further emphasizes
310 that excessive protease activity can contribute to the severity of periarticular
311 inflammation in *B. burgdorferi*-infected mice.
312
313 Previous research using serum, synovial fluid and tissue from Lyme arthritis
314 patients has been heavily focusing on innate and adaptive immune responses[7]. As a
315 result, limited data can be found regarding anti-protease and protease responses during

316 Lyme arthritis in human patients. In this study, we tested serum SLPI level in 5 healthy
317 subjects, 8 Lyme disease patients, 3 of whom had overt arthritis. We observed
318 decreased SLPI in the serum of these patients (Figure 4), suggesting an inverse
319 relationship between the SLPI level and *B. burgdorferi*-infection. However, a large
320 number of sera and synovial fluid samples from patients with Lyme arthritis and other
321 clinical manifestations of Lyme disease are needed to establish a definitive association.
322
323 *B. burgdorferi* first infects the skin of a vertebrate host following a tick bite, then
324 disseminates throughout the body, colonizes various tissue, evades immune responses,
325 and persists for a significant period of time. To survive the above processes, *B.*
326 *burgdorferi* interacts with various mammalian proteins, including decorin[41], fibronectin[42],
327 and plasminogen[43], among others. To comprehensively study the potential interaction
328 between *B. burgdorferi* and the host, our lab employed the BASEHIT (**BA**cterial
329 **S**election to **E**lucidate **H**ost-microbe **I**nteractions in high **T**hroughput) to assess the
330 interactions between *B. burgdorferi* and 3,336 human extracellular and secreted
331 proteins[44,46]. Using BASEHIT, our lab previously identified a strong interaction between
332 *B. burgdorferi* and Peptidoglycan Recognition Protein 1 (PGYRP1)[40]. Increased
333 infection burden in the heart and joint was observed in the mice lacking PGYRP1,
334 suggesting a role of PGYRP1 in the host response to *B. burgdorferi* infection.
335 Expanding the use of BASEHIT, CD55 was identified to bind *Borrelia crocidurae* and
336 *Borrelia persica*, two pathogens causing relapsing fever[45]. CD55-deficient mice infected
337 with *B. crocidurae* displayed lower pathogen load and elevated pro-inflammatory
338 cytokines. The above data demonstrate BASEHIT as an effective method to identify

339 host factors important in *B. burgdorferi* pathogenesis *in vivo*. In this study, we identified
340 an interaction between SLPI and *B. burgdorferi* using BASEHIT library screening and
341 subsequent flow cytometric analysis (Figure 5). The antimicrobial activity of SLPI has
342 been demonstrated against both gram-negative and positive bacteria including
343 *Escherichia coli*, *Pseudomonas aeruginosa*[49], *Mycobacteria tuberculosis*[50],
344 *Staphylococcus aureus*[51], and *Staphylococcus epidermidis*[49]. Interaction between the
345 positive charges of SLPI and the negative charges of bacteria surface, including
346 lipopolysaccharide (LPS), can destabilize bacteria cell wall leading to the bactericidal
347 effect[65]. *B. burgdorferi* do not have LPS[66] and this may account for the absence of the
348 bactericidal effect of SLPI against *B. burgdorferi* (Supplemental Figure 2A).
349
350 In conclusion, our data demonstrated the importance of SLPI in suppressing *B.*
351 *burgdorferi*-induced periarticular inflammation in mice by inhibiting recruitment of
352 neutrophils and macrophages and subsequent protease levels. We propose that, during
353 the active infection of the murine joint structures, the binding of *B. burgdorferi* with SLPI
354 depletes the local environment of SLPI. Such binding is specific to the infectious strain
355 of *B. burgdorferi.* As a potent anti-protease, the decrease in SLPI results in excessive
356 protease activity, including neutrophil elastase and MMP-8. These unchecked proteases
357 can lead to extensive tissue inflammation. Our study is the first to emphasize the
358 importance of an anti-protease-protease balance in the development of the periarticular
359 inflammation seen in *B. burgdorferi*-infected mice.
360

361 **Materials and methods**

362

363 **Sex as a biological variable**

364 Females *SLPI*-/- and WT C57BL/6 mice were used for the *in vivo B. burgdorferi*
365 infection. We have examined *B. burgdorferi* infection in both male and female C57BL/6
366 mice and no differences in the development of infection or disease have been noted.
367 Both male and female Lyme disease patients were included in the study. Sex was not
368 considered as a biological variable.

369

370 **Study approval**

371 This study used archived serum samples from adult Lyme disease subjects and
372 healthy controls that were previously collected under NIH U19AI089992 with approval of
373 the Yale University Institutional Review Board for human subjects research (IRB
374 protocol# 1112009475). All the animal experiments in this study were performed in
375 accordance with the Guidelines for the Care and Use of Laboratory Animals of the
376 National Institutes of Health. The animal protocols were approved by the Institutional
377 Animal Care and Use Committee at the Yale University School of Medicine.

378

379 **Measurement of serum SLPI levels in Lyme disease subjects and controls**

380 SLPI levels were measured in a total of 23 serum samples from 7 subjects at the
381 time of Lyme disease diagnosis (4 with a single erythema migrans lesion and 3 with the
382 late manifestation of Lyme arthritis) and from 5 healthy controls. Serum samples from
383 Lyme disease subjects were available at up to 3 times points: 1) study entry, range 0-9

384 days after onset of symptoms, 2) 30 days post diagnosis, and 3) up to 3 months after
385 completion of antibiotic therapy (range 4.5 – 6 months after dx). Additional details can
386 be found in Supplemental Table 1. The level of SLPI in the serum was measured using
387 the Human SLPI DuoSet ELISA kit (R&D Systems, #DY1274-05).
388
389 ***B. burgdorferi* culture**
390 *B. burgdorferi* B31-A3, an infectious clonal derivative of the sequenced strain
391 B31, was a generous gift from Dr. Utpal Pal at the Department of Veterinary Medicine,
392 University of Maryland, College Park[67]. *B. burgdorferi* B31-A3 and *B. burgdorferi* B31A
393 was grown in Barbour-Stoenner-Kelly H (BSK-H) complete medium (Sigma-Aldrich,
394 #B8291) in a 33°C setting incubator. The live cell density was determined by dark field
395 microscopy and using a hemocytometer (INCYTO, #DHC-N01). Low passage (P<3) *B.*
396 *burgdorferi* B31-A3 was used throughout this study.
397
398 ***In vivo* infection of mice**
399 The *SLPI*-/- C57BL/6 mice have been described previously[68,69]. The wild-type
400 (WT) C57BL/6 mice were purchased from the Jackson Laboratory and used as the
401 controls. 5 to 7 weeks of age female WT and *SLPI*-/- C57BL/6 mice were used for
402 infection. 4 to 6 weeks of age female C3H/HeN mice were purchased from Charles
403 River Laboratories and used for infection. Both C57BL/6 and C3H/HeN mice were
404 infected with low passage 10^5 *B. burgdorferi* subcutaneously (5–9 mice/group). PBS
405 sham-infected mice were used as controls. Ear punch biopsies were taken at 7-, 14-
406 and 21 to 28-day post-infection (dpi) to determine the infection burden in the skin. At 21-

407 28 dpi, mice were euthanized, and heart and joint tissues were collected to quantify the
408 spirochete burden. The protocol for the use of mice was reviewed and approved by the
409 Yale Animal Care and Use Committee.
410
411 **Quantification of *Borrelia* burden**
412 DNA was extracted from heart, tibiotarsal joint, and ear punch samples using
413 Qiagen DNeasy Blood & Tissue Kit, Qiagen. Quantitative PCR was performed using iQ-
414 SYBR Green Supermix (Bio-Rad). For quantitative detection of *B. burgdorferi* burden
415 within mouse tissue samples, q-PCR was performed with DNA using flagellin (*flaB*), a
416 marker gene for *Borrelia* detection. The mouse *β-actin* gene was used to normalize the
417 amount of DNA in each sample. The nucleotides sequences of primers used in specific
418 PCR applications are described previously[40].
419
420 **Joint histopathology analysis**
421 Mice were euthanized by CO_2 asphyxiation and one rear leg from each mouse
422 were dissected, immersion-fixed in Bouin's solution (Sigma-Aldrich, #HT10132). Fixed
423 tissues were embedded, sectioned, and stained with hematoxylin and eosin (HE) by
424 routine methods (Comparative Pathology Research Core in the Department of
425 Comparative Medicine, Yale School of Medicine). Periarticular and joint inflammation
426 was scored in a blinded fashion in a graded manner from 0 (negative), 1 (minimal), 2
427 (moderate), to 3 (severe).
428
429 **Flow cytometry to quantify infiltrating cells in joint tissues in mice**

430 The WT and *SLPI*-/- C57BL/6 mice were infected with *B. burgdorferi* as described
431 above. The mice were euthanized 21-28 dpi. The ankle joints were cut out at around 0.7
432 cm proximal to the ankle joint. The portion distal to the midfoot was discarded, and the
433 skin removed. The bone marrow cells were flushed out with RPMI 1640 (Gibco, #11875-
434 093) using a 27-gauge needle. The bone marrow-depleted ankles were cut into 3-4 mm
435 sized tissue pieces and incubated with digestion media containing
436 2.4 mg/ml hyaluronidase (Sigma-Aldrich, #H3506), 1 mg/ml collagenase (Sigma-Aldrich,
437 #C2139) in RPMI 1640 (Gibco, #11875-093) supplemented with 10% fetal bovine serum
438 (FBS) for 1 h at 37 °C with 5%CO_2. The digestion media containing the tissue pieces
439 were passed through a 70 µm cell strainer (Thermo Scientific, #352350). The remaining
440 tissue pieces were mashed using a 10 ml syringe plunger. The digestion media
441 containing the isolated cells were neutralized with RPMI 1640 with 10% FBS[35]. The red
442 blood cells were lysed by ACK Lysing buffer (Gibco, #A1049201). The cells were rinsed
443 and resuspended in FACS buffer and ready for staining for flow cytometry.
444
445 The cells were incubated with Fc receptor antibody (TruStain FcXTM anti-mouse
446 CD16/32) (BioLegend, #101320), and antibodies including PerCP anti-mouse CD45
447 (BioLegend, #103130), BV711 anti-mouse Ly6G (BioLegend, #127643), PE anti-mouse
448 CD11b (BioLegend, #101208), APC/CY7 anti-mouse CX3CR21 (BioLegend, #149047),
449 FITC anti-mouse Ly6C (BioLegend, #128005), APC anti-mouse CD64 (BioLegend,
450 #139305) and LIVE/DEADTM fixable violet stain kit (Invitrogen, #L34955) on ice for 30
451 min. The samples were rinsed twice with FACS buffer and run through BD LSRII (BD
452 bioscience). The data was then analyzed by FlowJo[36].

453

454 **Gene expression evaluation by quantitative real-time PCR**

455 Mice were euthanized at 21-28 dpi. The ankle joints were excised as described
456 above, snap-frozen in liquid nitrogen, and stored at −80°C. The frozen tissue was
457 pulverized in liquid nitrogen using a mortar and pestle[70]. The RNA was purified using
458 Trizol (Invitrogen, #15596-018) following a published protocol[71]. cDNA was synthesized
459 using the iScript cDNA Synthesis Kits (Bio-Rad, #1708891). qPCR was performed using
460 iQ SYBR Green Supermix (Bio-Rad, #1725124). The relative expression of each target
461 gene was normalized to the mouse *β-actin* gene. The target genes and corresponding
462 primer sequences are shown in the Key Resource Table.

463

464 **Murine neutrophil elastase, cytokine, chemokine, and MMP profile**

465 Blood samples from each group of mice was collected by cardiac puncture at 21-
466 28 dpi and sera were collected. The murine neutrophil elastase level was measured
467 using the Mouse Neutrophil Elastase/ELA2 DuoSet ELISA (RnD Systems, #DY4517-
468 05). Serum was sent for cytokine analysis by the Mouse Cytokine/Chemokine 32-Plex
469 Discovery Assay Array (MD32), and the Mouse MMP 5-Plex Discovery Assay Array
470 (MDMMP-S, P) performed by Eve Technologies. The cytokines and chemokines
471 represented by MD32 are Eotaxin, G-CSF, GM-CSF, IFN-γ, IL-1α, IL-1β, IL-2, IL-3, IL-4,
472 IL-5,IL-6, IL-7, IL-9, IL-10, IL-12 (p40), IL-12 (p70), IL-13, IL-15, IL-17A, IP-10, KC, LIF,
473 LIX, MCP-1, M-CSF, MIG, MIP-1α, MIP-1β, MIP-2, RANTES, TNFα, and VEGF. The
474 MMPs represented by MDMMP-S, P are MMP-2, MMP-3, MMP-8, proMMP-9, and
475 MMP-12.

476

477 **Purification of recombinant murine SLPI**

478 The murine *SLPI* cDNA ORF clone was purchased from GenScript (OMu22721).
479 The coding sequence was subsequently cloned into pET22b(+) expression vector
480 (Novagen) in frame with the pelB signal peptide using Gibson Assembly[72]. *E. coli* strain
481 Rosetta-gami 2 (DE3) (Novagen, #71351) was transformed with the SLPI-pET22b+ and
482 grown at 37°C with ampicillin (100 µg/ml), tetracycline (12.5 µg/ml), streptomycin (50
483 µg/ml) and chloramphenicol (34 µg/ml). Cells were induced with 1 mM IPTG (18°C,
484 overnight), harvested, and lysed with BugBuster Protein Extraction Reagent (Novagen,
485 #70921-3). Recombinant mSLPI was purified with a Ni-NTA resin column as described
486 by the manufacturer (Qiagen). To evaluate the activity of the purified rmSLPI, the trypsin
487 inhibitory activity was assayed with the fluorescent substrate Mca-RPKPVE-Nval-
488 WRK(Dnp)-NH2 Fluorogenic MMP Substrate (R&D Systems, #ES002) and the
489 absorbance was monitored at 405 nm using a fluorescent plate reader (Tecan).

490

491 **Flow cytometry to validate *B. burgdorferi*-SLPI binding**

492 Low passage *B. burgdorferi* was cultured to a density of 10^6–10^7 cells/ml and
493 harvested at 10,000 g for 10 min. Cells were rinsed twice with PBS and blocked in
494 1%BSA for 1 h at 4°C. The cells were pelleted, rinsed, resuspended, and incubated with
495 10 nM and 1 µM human SLPI (R&D Systems, #1274-PI-100) and murine SLPI
496 (produced in lab as described above) at 4°C for 2 h. The binding was detected with goat
497 anti human or murine SLPI (R&D Systems, #AF1274 and AF1735) and Alexa Fluor 488
498 or Alexa Fluor 647 donkey anti goat IgG (H+L) (Invitrogen, #A32814, A-21447). The

499 samples were fixed with 2% PFA before running through BD LSRII Green (BD
500 bioscience). The data was then analyzed by FlowJo.
501
502 **ELISA to validate *B. burgdorferi*-SLPI binding**
503 *B. burgdorferi* was cultured to a density of 10^6–10^7 cells/ml and harvested at
504 10,000 g for 10 min. To make the *B. burgdorferi* lysate, cells were rinsed twice with PBS,
505 pelleted, and lysed using BugBuster Protein Extraction Reagent (Novagen, #70921-3).
506 Protein concentration in the lysate was measured by absorbance at 280 nm using the
507 nanodrop (Fisher Scientific). For the protease assay, the *B. burgdorferi* lysate was
508 incubated in the presence or absence of proteinase K (0.2 mg/ml, Thermo Scientific,
509 #EO0491) for 10 min. In an immuno 96-well plate (MaxiSorp), wells were coated with
510 200 ng of *B. burgdorferi* lysate. Samples were blocked with 1% BSA followed by
511 incubation with human SLPI at varying concentrations (1–1000 ng) for 1 h at room
512 temperature. The binding was probed with goat anti human SLPI (R&D Systems,
513 #AF1274) and rabbit anti goat IgG (whole molecule)-Peroxidases antibody (Sigma-
514 Aldrich, #A8919-2ML). KPL Sureblue TMB Microwell Peroxidase substrate, 1-
515 component (Seracare, #5120-0077) was used. The reaction was stopped with KPL TMB
516 stop solution (Seracare, #5150-0021), and absorbance was read at 450 nm.
517
518 **Immunofluorescence assay**
519 *B. burgdorferi* was cultured to a density of 10^6–10^7 cells/ml, rinsed twice with
520 PBS and blocked with 1% BSA for 1 h at 4°C. *B. burgdorferi* was incubated with human
521 or murine SLPI at 4°C for 2 h. The spirochetes were probed with goat anti human or

522 murine SLPI (R&D Systems, #AF1274 and AF1735) and Alexa Fluor 488 donkey anti
523 goat IgG (H+L) (Invitrogen, #A32814). *B. burgdorferi* were then stained with Hoechst
524 33342 (Invitrogen, #H1399). The samples were fixed with in 2% PFA before imaged with
525 Leica SP8.
526

527 **The BacTiter Glo microbial cell viability assay to quantify *B. burgdorferi* viability**

528 The BacTiter Glo microbial cell viability assay quantifies the ATP present in the
529 microbial culture by measuring luminescence. The amount of ATP is proportional to the
530 number of viable cells in culture[40,45,73]. To test the borreliacidal activity of human SLPI,
531 $1x10^5$ spirochetes were treated with 0–10 μM hSLPI (R&D Systems, #1274-PI-100) at
532 33°C for 48 h. The luminescence was measured using a fluorescence plate reader
533 (Tecan). The percent viability was normalized to the control spirochetes culture without
534 hSLPI treatment. To test the effect of hSLPI on the antibody-mediated *B. burgdorferi*
535 killing, $1x10^5$ spirochetes were pretreated with 0–5 μM hSLPI (R&D Systems, #1274-PI-
536 100) at 33°C for 2 h. 20% mouse *B. burgdorferi* antisera were then added and
537 incubated for 2 and 4 h. The mouse antisera were collected from *B. burgdorferi* infected
538 mice at 28 dpi. The luminescence was measured as described above. The percent
539 viability was normalized to the control spirochetes culture without any treatment.
540

541 **Statistical analysis**

542 The analysis of all data was performed using the non-parametric Mann-Whitney,
543 or ANOVA using Prism 10 software (GraphPad Software, Inc., San Diego, CA). A *p*-
544 value of <0.05 was considered statistically significant.

545

546 **ACKNOWLEGMENTS**

547

548 We are grateful to Dr. Narasimhan for her input and suggestions during
549 experiment design, and to Dr. Ming-Jie Wu for his assistance in conducting
550 experiments. We are grateful to Ms. Ming Li for her effort in preparing human sera
551 samples. This work was supported by NIH grants AI165499 and AI138949, the Steven
552 and Alexandra Cohen Foundation, and the Howard Hughes Medical Institute Emerging
553 Pathogens Initiative.

554

555 **AUTHOR CONTRIBUTIONS**

556

557 QY and EF designed, performed, and analyzed experiments and draft the
558 manuscript. XT designed and performed experiments. TH performed the BASEHIT
559 library screen. RH scored the severity of murine ankle inflammation. AB and LB
560 provided sera from Lyme disease patients and edited the manuscript. AN provided the
561 *SLPI*-/- mice. AR developed the BASEHIT screen. EF scored the visual swelling level of
562 murine tibiotarsal joints and supervised the research.

563

564 **Figure Legends**

565

566 **Figure 1. *B. burgdorferi* burden in C57BL/6 WT and *SLPI*-/- mice.** WT and *SLPI*-/-
567 mice were infected with 10^5 spirochetes by subcutaneous injection. (A-C) Spirochete

568 burden in skin was assessed by ear punch biopsies at 7d (A) 14 d (B), and 21-28 d (C)
569 post infection. (D and E) Spirochete burden in tibiotarsal joint and heart tissues was
570 assessed at 21-28 d (D, heart, E, joint) post infection. At least n = 6 mice were infected
571 in each group. The spirochete burden was measured by qPCR detecting *flaB* and
572 normalized to mouse *β-actin*. Each data point represents an individual animal.
573 Representative data were shown from three separate experiments. The error bars
574 represent mean ± SEM and *p*-values are calculated using the non-parametric Mann-
575 Whitney test.
576
577 **Figure 2. Assessment of ankle inflammation in WT and *SLPI*-/- mice infected with**
578 ***B. burgdorferi* at 21-28 dpi.** (A) Representative images are shown of the tibiotarsal
579 joints of WT and *SLPI*-/- mice with/without *B. burgdorferi* infection at 21-28 dpi. The
580 swelling is indicated by the red arrow. (B) Swelling of the tibiotarsal joints of individual
581 mice was scored visually by an observer blinded to the experimental groups (scale of 0
582 (negative) to 3 (severe)). (C) The tibiotarsal joint of each mouse was dissected, fixed,
583 sectioned, and stained with H&E. Representative images from *B. burgdorferi*-infected
584 C57BL/6 WT and *SLPI*-/- mice are shown. Lower magnification (left panels, Scale bar:
585 100 μm) and higher magnification (right panels, Scale bar: 50 μm) of selected areas
586 (black rectangle) are shown. (D) The severity of periarticular inflammation was scored
587 blindly by the pathologist on a scale of 0 (negative) to 3 (severe). Infected animals are
588 shown in red. None of the mice exhibited synovial inflammation. Results from two
589 independent experiments were pooled and shown here. The error bars represent mean
590 ± SEM and *p*-values are calculated using the non-parametric Mann-Whitney test.

591

592 **Figure 3. Immune profile analysis of infected WT and *SLPI*-/- mice.** (A, B) Infiltrating
593 cell population analysis of tibiotarsal joint tissues of infected WT and *SLPI*-/- mice. (A)
594 The neutrophil population was gated on the CD11bLY6G double positive cells among
595 the CD45 positive cells. (B) The macrophage population was gated on the CD64
596 positive cells among the CX3CR1 positive myeloid cells. Results from two independent
597 experiments were pooled and shown here. (C-E) Expression levels of CXCR2 (C),
598 MCP-1 (D), and CCR2 (E) were assessed in the tibiotarsal tissue using RT-qPCR. (F)
599 The serum cytokine profile was assess using mouse cytokine/chemokine 32-plex array.
600 An increase in IL-6 was observed in the infected *SLPI*-/- mice. (G, H) The serum level of
601 neutrophil elastase (NE) was measured using an ELISA kit. (I) Serum levels of MMPs
602 were assessed using a mouse MMP 5-Plex Discovery Assay. An increase in MMP-8
603 was observed in the infected *SLPI*-/- mice. Serum was obtained by cardiac puncture of
604 WT and *SLPI*-/- C57BL/6 mice with/without infection at 21-28 dpi (F, G, and I) and of
605 infected C3H/HeN mice at 21 dpi (H). black, PBS-sham infection; red, *B. burgdorferi*
606 infection. Each data point represents an individual animal. The error bar represents
607 mean ± SEM and *p*-values are calculated using the non-parametric Mann-Whitney test.

608

609 **Figure 4. Serum SLPI levels in Lyme disease subjects versus healthy controls.**
610 The serum level of SLPI was measured by ELISA. Sera samples were from 5 adult
611 healthy controls (HC). 18 samples were from people with Lyme disease (LD) including 5
612 samples from 3 subjects presenting with Lyme arthritis (red) and 13 samples from 4

613 subjects with erythema migrans (black). The error bar represents mean ± SEM and *p*-
614 values are calculated using the non-parametric Mann-Whitney test.
615
616 **Figure 5. *B. burgdorferi* interaction with human and murine SLPI.** (A) Sandwich
617 ELISA results show the interaction of *B. burgdorferi* whole cell lysates with human SLPI.
618 ELISA plates were coated with *B. burgdorferi* whole cell lysates and probed with
619 increasing amount of human SLPI (blue) or human Fc proteins (black) as the negative
620 control. The values plotted represent the mean ± SEM of duplicates from two
621 experiments. *P*-value is displayed in the graph and determined using the non-
622 parametric Mann-Whitney test. (B and C) Flow cytometry histograms show binding of
623 human (B) and murine (C) SLPI to *B. burgdorferi* cultured at 33°C (solid line) and 37°C
624 (dash line). *B. burgdorferi* was cultured to a density of 10^6/ml. The same volume of
625 cultures was incubated at 33°C or 37°C for 24 hrs before adding 10 nM (green) or 1 μM
626 (red) human or murine SLPI. The binding was detected with goat anti human or murine
627 SLPI and donkey anti goat AF647 or AF488. *B. burgdorferi* alone (grey) and antibody
628 control (blue) were used as negative controls. (D) Immuno-fluorescent microscopy was
629 used to directly observe the binding of *B. burgdorferi* with human and murine SLPI.
630 Merged and single-color images are shown. Scale bar: 10 μm.
631
632 **Supplemental Figure 1. The binding of human SLPI to non-infectious *B.***
633 ***burgdorferi* and proteinase K-treated *B. burgdorferi*.** (A) Flow cytometry histogram
634 shows the lack of binding of human SLPI (1 μM, red) to non-infectious *B. burgdorferi*
635 *B31A. B. burgdorferi* alone (grey) and antibody control (blue) were used as negative

636 controls. (B) ELISA result shows the interaction between human SLPI and *B. burgdorferi*
637 whole cell lysates in the presence (blue) or absence (black) of proteinase K. ELISA
638 plates were coated with *B. burgdorferi* whole cell lysates and probed with increasing
639 amount of human SLPI. The values plotted represent the mean ± SEM of triplicates
640 from one experiment.
641
642 **Supplemental Figure 2. The effect of human SLPI binding on *B. burgdorferi***
643 **viability and antibody-mediated killing.** (A) Human SLPI (hSLPI, 0-10 μM) was
644 incubated with 10^5 *B. burgdorferi* at 33°C for 48 hours. The viability was assessed by
645 BacTiter Glo microbial cell viability assay. The percent viability was normalized to the
646 control spirochetes culture without hSLPI treatment. Results from one independent
647 experiment performed in triplicate samples are shown here. (B) Human SLPI (hSLPI, 0-
648 5 μM) was incubated with 10^5 *B. burgdorferi* at 33°C for 2 hours. 20% mouse *B.*
649 *burgdorferi* antisera were then added for 2 and 4 h. The viability was measured as
650 described above. The percent viability was normalized to the control spirochetes culture
651 without any treatment. Results from two independent experiments performed in
652 duplicate samples are shown here.
653
654 **Supplemental Table 1. Subject Characterization**
655
656 **Supplemental Table 2. The primers used in this study.**
657
658 **Key resources table**

659

Reagent type (species) or resource	Designation	Source or reference	IDENTIFIER
Antibodies	TruStain FcXTM anti-mouse CD16/32	BioLegend	Cat#101320
Antibodies	PerCP anti-mouse CD45	BioLegend	Cat#103130
Antibodies	BV711 anti-mouse Ly6G	BioLegend	Cat#127643
Antibodies	PE anti-mouse CD11b	BioLegend	Cat#101208
Antibodies	APC/CY7 anti-mouse CX3CR21	BioLegend	Cat#149047
Antibodies	FITC anti-mouse Ly6C	BioLegend	Cat#128005
Antibodies	APC anti-mouse CD64	BioLegend	Cat#139305
Antibodies	goat anti human SLPI	R&D Systems	Cat#AF1274
Antibodies	goat anti murine SLPI	R&D Systems	Cat#AF1735
Antibodies	Alexa Fluor 488 donkey anti goat IgG (H+L)	Invitrogen	Cat#A32814
Antibodies	Alexa Fluor 647 donkey anti goat IgG (H+L)	Invitrogen	Cat#A-21447
Bacterial strains	*Borrelia. burgdorferi* B31-A3	Dr. Utpal Pal's laboratory	N/A
Bacterial strains	*Borrelia. burgdorferi* B31-A	This manuscript	N/A
Bacterial strains	*E. coli* Rosetta-gami 2 (DE3) competent cell	Novagen	Cat#71351
Biological samples	Mouse tibiotarsal tissue	This manuscript	N/A
Recombinant proteins	human SLPI	R&D Systems	Cat#1274-PI-100
Chemical	iQ SYBR Green Supermix	Bio-Rad	Cat#1725124
Chemical	Barbour-Stoenner-Kelly H (BSK-H) complete medium	Sigma-Aldrich	Cat#B8291
Chemical	Bouin's solution	Sigma-Aldrich	Cat#HT10132
Chemical	Hyaluronidase	Sigma-Aldrich	Cat#H3506
Chemical	Collagenase	Sigma-Aldrich	Cat#C2139
Chemical	ACK Lysing buffer	Gibco	Cat#A1049201
Chemical	Trizol	Invitrogen,	Cat#15596-018
peptide	Mca-RPKPVE-Nval-WRK(Dnp)-NH2 Fluorogenic MMP Substrate	R&D Systems	Cat#ES002
Chemical	BugBuster Protein Extraction Reagent	Novagen	Cat#70921-3
Chemical	Proteinase K	Thermo Scientific	Cat#EO0491
Chemical	Ni-NTA agarose	QIAGEN	Cat#30230
Chemical	KPL Sureblue TMB Microwell Peroxidase substrate, 1-component	Seracare	Cat#5120-0077
Chemical	KPL TMB stop solution	Seracare	Cat#5150-0021
Chemical	Hoechst 33342	Invitrogen	Cat#H1399

Chemical	RPMI 1640	Gibco	Cat#11875-093
Critical commercial assays	LIVE/DEADTM fixable violet stain kit	Invitrogen	Cat#L34955
Critical commercial assays	iScript cDNA Synthesis Kit	Bio-Rad	Cat#1708891
Critical commercial assays	DNeasy Blood & Tissue Kit	Qiagen	
Critical commercial assays	Gibson Assembly Kit	NEB	
Critical commercial assays	Mouse Neutrophil Elastase/ELA2 DuoSet ELISA	RnD Systems	Cat#DY4517-05
Critical commercial assays	Human SLPI DuoSet ELISA	RnD Systems	Cat#DY1274-05
Critical commercial assays	BacTiter-Glo Microbial Cell Viability Assay kit	Promega	Cat#G8230
Critical commercial assays	Mouse MMP 5-Plex Discovery Assay Array (MDMMP-S, P)	Eve Technologies	N/A
Critical commercial assays	Mouse Cytokine/Chemokine 32-Plex Discovery Assay Array (MD32)	Eve Technologies	N/A
Experimental models: Organisms/strains	*SLPI-/-* mice	Dr. Akira Nakamura's laboratory[68, 69]	https://doi.org/10.3389/fimmu.2017.01538 https://doi.org/10.1084/jem.20021824
Experimental models: Organisms/strains	C3H/HeN mice	Charles River Laboratories	N/A
Experimental models: Organisms/strains	C57BL/6 mice	Jackson Laboratory	Stock #: 000664; RRID: IMSR_JAX:000664
Recombinant DNA	Plasmid: Murine *SLPI* cDNA ORF clone	GenScript	OMu22721
Recombinant DNA	Plasmid: pET-22b (+)	Novagen	Cat#69744-3
Software and algorithms	Prism	GraphPad	RRID:SCR_002798
Software and algorithms	FlowJo	BD Biosciences	https://www.flowjo.com/

663 **References**

664 1. Kugeler, K.J., Schwartz, A.M., Delorey, M.J., Mead, P.S., and Hinckley, A.F.
665 (2021). Estimating the frequency of Lyme disease diagnoses, United States,
666 2010–2018. Emerging Infectious Diseases *27*, 616.
667 2. Mead, P. (2022). Epidemiology of Lyme Disease. Infect Dis Clin North Am *36*,
668 495-521. 10.1016/j.idc.2022.03.004.
669 3. Arvikar, S.L., and Steere, A.C. (2022). Lyme arthritis. Infectious Disease Clinics
670 *36*, 563-577.
671 4. Schwartz, A.M., Hinckley, A.F., Mead, P.S., Hook, S.A., and Kugeler, K.J. (2017).
672 Surveillance for Lyme Disease - United States, 2008-2015. MMWR Surveill
673 Summ *66*, 1-12. 10.15585/mmwr.ss6622a1.
674 5. Steere, A.C., Schoen, R.T., and Taylor, E. (1987). The clinical evolution of Lyme
675 arthritis. Ann Intern Med *107*, 725-731. 10.7326/0003-4819-107-5-725.
676 6. Miller, J.B., and Aucott, J.N. (2021). Stages of Lyme Arthritis. J Clin Rheumatol
677 *27*, e540-e546. 10.1097/RHU.0000000000001513.
678 7. Lochhead, R.B., Strle, K., Arvikar, S.L., Weis, J.J., and Steere, A.C. (2021). Lyme
679 arthritis: linking infection, inflammation and autoimmunity. Nature Reviews
680 Rheumatology *17*, 449-461.
681 8. Shin, J.J., Glickstein, L.J., and Steere, A.C. (2007). High levels of inflammatory
682 chemokines and cytokines in joint fluid and synovial tissue throughout the course
683 of antibiotic-refractory lyme arthritis. Arthritis Rheum *56*, 1325-1335.
684 10.1002/art.22441.
685 9. Lochhead, R.B., Ordoñez, D., Arvikar, S.L., Aversa, J.M., Oh, L.S., Heyworth, B.,
686 Sadreyev, R., Steere, A.C., and Strle, K. (2019). Interferon-gamma production in
687 Lyme arthritis synovial tissue promotes differentiation of fibroblast-like
688 synoviocytes into immune effector cells. Cell Microbiol *21*, e12992.
689 10.1111/cmi.12992.
690 10. Gross, D.M., Steere, A.C., and Huber, B.T. (1998). T helper 1 response is
691 dominant and localized to the synovial fluid in patients with Lyme arthritis. J
692 Immunol *160*, 1022-1028.
693 11. Lochhead, R.B., Arvikar, S.L., Aversa, J.M., Sadreyev, R.I., Strle, K., and Steere,
694 A.C. (2019). Robust interferon signature and suppressed tissue repair gene
695 expression in synovial tissue from patients with postinfectious, Borrelia
696 burgdorferi-induced Lyme arthritis. Cell Microbiol *21*, e12954. 10.1111/cmi.12954.
697 12. Barthold, S.W., Beck, D.S., Hansen, G.M., Terwilliger, G.A., and Moody, K.D.
698 (1990). Lyme borreliosis in selected strains and ages of laboratory mice. J Infect
699 Dis *162*, 133-138. 10.1093/infdis/162.1.133.
700 13. Barthold, S.W. (1996). Lyme borreliosis in the laboratory mouse.
701 14. Ma, Y., Seiler, K.P., Eichwald, E.J., Weis, J.H., Teuscher, C., and Weis, J.J.
702 (1998). Distinct characteristics of resistance to Borrelia burgdorferi-induced
703 arthritis in C57BL/6N mice. Infect Immun *66*, 161-168. 10.1128/IAI.66.1.161-
704 168.1998.
705 15. Brown, C.R., and Reiner, S.L. (1999). Genetic control of experimental Lyme
706 arthritis in the absence of specific immunity. Infection and immunity *67*, 1967-
707 1973.

708 16. Ritzman, A.M., Hughes-Hanks, J.M., Blaho, V.A., Wax, L.E., Mitchell, W.J., and
709 Brown, C.R. (2010). The chemokine receptor CXCR2 ligand KC (CXCL1)
710 mediates neutrophil recruitment and is critical for development of experimental
711 Lyme arthritis and carditis. Infect Immun *78*, 4593-4600. 10.1128/IAI.00798-10.
712 17. Miller, J.C., Ma, Y., Bian, J., Sheehan, K.C., Zachary, J.F., Weis, J.H., Schreiber,
713 R.D., and Weis, J.J. (2008). A critical role for type I IFN in arthritis development
714 following Borrelia burgdorferi infection of mice. J Immunol *181*, 8492-8503.
715 10.4049/jimmunol.181.12.8492.
716 18. Brown, C.R., Blaho, V.A., and Loiacono, C.M. (2003). Susceptibility to
717 experimental Lyme arthritis correlates with KC and monocyte chemoattractant
718 protein-1 production in joints and requires neutrophil recruitment via CXCR2. J
719 Immunol *171*, 893-901. 10.4049/jimmunol.171.2.893.
720 19. Anguita, J., Barthold, S.W., Persinski, R., Hedrick, M.N., Huy, C.A., Davis, R.J.,
721 Flavell, R.A., and Fikrig, E. (2002). Murine Lyme arthritis development mediated
722 by p38 mitogen-activated protein kinase activity. J Immunol *168*, 6352-6357.
723 10.4049/jimmunol.168.12.6352.
724 20. Doumas, S., Kolokotronis, A., and Stefanopoulos, P. (2005). Anti-inflammatory
725 and antimicrobial roles of secretory leukocyte protease inhibitor. Infect Immun *73*,
726 1271-1274. 10.1128/IAI.73.3.1271-1274.2005.
727 21. Thompson, R.C., and Ohlsson, K. (1986). Isolation, properties, and complete
728 amino acid sequence of human secretory leukocyte protease inhibitor, a potent
729 inhibitor of leukocyte elastase. Proc Natl Acad Sci U S A *83*, 6692-6696.
730 10.1073/pnas.83.18.6692.
731 22. Moreau, T., Baranger, K., Dadé, S., Dallet-Choisy, S., Guyot, N., and Zani, M.L.
732 (2008). Multifaceted roles of human elafin and secretory leukocyte proteinase
733 inhibitor (SLPI), two serine protease inhibitors of the chelonianin family. Biochimie
734 *90*, 284-295. 10.1016/j.biochi.2007.09.007.
735 23. Maruyama, M., Hay, J.G., Yoshimura, K., Chu, C.S., and Crystal, R.G. (1994).
736 Modulation of secretory leukoprotease inhibitor gene expression in human
737 bronchial epithelial cells by phorbol ester. J Clin Invest *94*, 368-375.
738 10.1172/JCI117331.
739 24. Sallenave, J.M., Shulmann, J., Crossley, J., Jordana, M., and Gauldie, J. (1994).
740 Regulation of secretory leukocyte proteinase inhibitor (SLPI) and elastase-
741 specific inhibitor (ESI/elafin) in human airway epithelial cells by cytokines and
742 neutrophilic enzymes. Am J Respir Cell Mol Biol *11*, 733-741.
743 10.1165/ajrcmb.11.6.7946401.
744 25. Ashcroft, G.S., Lei, K., Jin, W., Longenecker, G., Kulkarni, A.B., Greenwell-Wild,
745 T., Hale-Donze, H., McGrady, G., Song, X.Y., and Wahl, S.M. (2000). Secretory
746 leukocyte protease inhibitor mediates non-redundant functions necessary for
747 normal wound healing. Nat Med *6*, 1147-1153. 10.1038/80489.
748 26. Zhu, J., Nathan, C., Jin, W., Sim, D., Ashcroft, G.S., Wahl, S.M., Lacomis, L.,
749 Erdjument-Bromage, H., Tempst, P., Wright, C.D., and Ding, A. (2002).
750 Conversion of proepithelin to epithelins: roles of SLPI and elastase in host
751 defense and wound repair. Cell *111*, 867-878. 10.1016/s0092-8674(02)01141-8.
752 27. Taggart, C.C., Cryan, S.A., Weldon, S., Gibbons, A., Greene, C.M., Kelly, E.,
753 Low, T.B., O'neill, S.J., and McElvaney, N.G. (2005). Secretory leucoprotease

754 inhibitor binds to NF-kappaB binding sites in monocytes and inhibits p65 binding.
755 J Exp Med *202*, 1659-1668. 10.1084/jem.20050768.
756 28. Taggart, C.C., Greene, C.M., McElvaney, N.G., and O'Neill, S. (2002). Secretory
757 leucoprotease inhibitor prevents lipopolysaccharide-induced IkappaBalpha
758 degradation without affecting phosphorylation or ubiquitination. J Biol Chem *277*,
759 33648-33653. 10.1074/jbc.M203710200.
760 29. Jin, F.Y., Nathan, C., Radzioch, D., and Ding, A. (1997). Secretory leukocyte
761 protease inhibitor: a macrophage product induced by and antagonistic to
762 bacterial lipopolysaccharide. Cell *88*, 417-426. 10.1016/s0092-8674(00)81880-2.
763 30. Huet, G., Flipo, R.M., Richet, C., Thiebaut, C., Demeyer, D., Balduyck, M.,
764 Duquesnoy, B., and Degand, P. (1992). Measurement of elastase and cysteine
765 proteinases in synovial fluid of patients with rheumatoid arthritis, sero-negative
766 spondylarthropathies, and osteoarthritis. Clin Chem *38*, 1694-1697.
767 31. Wilkinson, D.J., Arques, M.D.C., Huesa, C., and Rowan, A.D. (2019). Serine
768 proteinases in the turnover of the cartilage extracellular matrix in the joint:
769 implications for therapeutics. Br J Pharmacol *176*, 38-51. 10.1111/bph.14173.
770 32. McDonnell, J., Lobner, J.M., Knight, W.B., Lark, M.W., Green, B., Poe, M., and
771 Moore, V.L. (1993). Comparison of the proteoglycanolytic activities of human
772 leukocyte elastase and human cathepsin G in vitro and in vivo. Connect Tissue
773 Res *30*, 1-9. 10.3109/03008209309032926.
774 33. Lee, S.-Y., Nho, T.-H., Choi, B.-D., Jeong, S.-J., Lim, D.-S., and Jeong, M.-J.
775 (2016). Secretory leukocyte protease inhibitor reduces inflammation and alveolar
776 bone resorption in LPS-induced periodontitis in rats and in MC3T3-E1
777 preosteoblasts. Animal Cells and Systems *20*, 344-352.
778 10.1080/19768354.2016.1250817.
779 34. Song, X., Zeng, L., Jin, W., Thompson, J., Mizel, D.E., Lei, K., Billinghurst, R.C.,
780 Poole, A.R., and Wahl, S.M. (1999). Secretory leukocyte protease inhibitor
781 suppresses the inflammation and joint damage of bacterial cell wall-induced
782 arthritis. J Exp Med *190*, 535-542. 10.1084/jem.190.4.535.
783 35. Akitsu, A., and Iwakura, Y. (2016). Isolation of Joint-infiltrating Cells. Bio-protocol
784 *6*, e1911-e1911.
785 36. Feng, G., Zhu, C., Lin, C.Y., Bredemeyer, A., Förster, I., Kreisel, D., and Lavine,
786 K.J. (2023). CCL17 Protects Against Viral Myocarditis by Suppressing the
787 Recruitment of Regulatory T Cells. J Am Heart Assoc *12*, e028442.
788 10.1161/JAHA.122.028442.
789 37. Srirangan, S., and Choy, E.H. (2010). The role of interleukin 6 in the
790 pathophysiology of rheumatoid arthritis. Ther Adv Musculoskelet Dis *2*, 247-256.
791 10.1177/1759720X10378372.
792 38. Murphy, G., and Nagase, H. (2008). Reappraising metalloproteinases in
793 rheumatoid arthritis and osteoarthritis: destruction or repair? Nat Clin Pract
794 Rheumatol *4*, 128-135. 10.1038/ncprheum0727.
795 39. Hu, L.T., Eskildsen, M.A., Masgala, C., Steere, A.C., Arner, E.C., Pratta, M.A.,
796 Grodzinsky, A.J., Loening, A., and Perides, G. (2001). Host metalloproteinases in
797 Lyme arthritis. Arthritis Rheum *44*, 1401-1410. 10.1002/1529-
798 0131(200106)44:6<1401::AID-ART234>3.0.CO;2-S.

40. Gupta, A., Arora, G., Rosen, C.E., Kloos, Z., Cao, Y., Cerny, J., Sajid, A., Hoornstra, D., Golovchenko, M., Rudenko, N., et al. (2020). A human secretome library screen reveals a role for Peptidoglycan Recognition Protein 1 in Lyme borreliosis. PLoS Pathog *16*, e1009030. 10.1371/journal.ppat.1009030.
41. Shi, Y., Xu, Q., McShan, K., and Liang, F.T. (2008). Both decorin-binding proteins A and B are critical for the overall virulence of Borrelia burgdorferi. Infect Immun *76*, 1239-1246. 10.1128/IAI.00897-07.
42. Li, X., Liu, X., Beck, D.S., Kantor, F.S., and Fikrig, E. (2006). Borrelia burgdorferi lacking BBK32, a fibronectin-binding protein, retains full pathogenicity. Infect Immun *74*, 3305-3313. 10.1128/IAI.02035-05.
43. Koenigs, A., Hammerschmidt, C., Jutras, B.L., Pogoryelov, D., Barthel, D., Skerka, C., Kugelstadt, D., Wallich, R., Stevenson, B., Zipfel, P.F., and Kraiczy, P. (2013). BBA70 of Borrelia burgdorferi is a novel plasminogen-binding protein. J Biol Chem *288*, 25229-25243. 10.1074/jbc.M112.413872.
44. Sonnert, N.D., Rosen, C.E., Ghazi, A.R., Franzosa, E.A., Duncan-Lowey, B., González-Hernández, J.A., Huck, J.D., Yang, Y., Dai, Y., Rice, T.A., et al. (2024). A host-microbiota interactome reveals extensive transkingdom connectivity. Nature *628*, 171-179. 10.1038/s41586-024-07162-0.
45. Arora, G., Lynn, G.E., Tang, X., Rosen, C.E., Hoornstra, D., Sajid, A., Hovius, J.W., Palm, N.W., Ring, A.M., and Fikrig, E. (2022). CD55 Facilitates Immune Evasion by Borrelia crocidurae, an Agent of Relapsing Fever. mBio *13*, e0116122. 10.1128/mbio.01161-22.
46. Hart, T.M., Sonnert, N.D., Tang, X., Chaurasia, R., Allen, P.E., Hunt, J.R., Read, C.B., Johnson, E.E., Arora, G., Dai, Y., et al. (2024). An atlas of human vector-borne microbe interactions reveals pathogenicity mechanisms. Cell. 10.1016/j.cell.2024.05.023.
47. Caine, J.A., and Coburn, J. (2015). A short-term Borrelia burgdorferi infection model identifies tissue tropisms and bloodstream survival conferred by adhesion proteins. Infect Immun *83*, 3184-3194. 10.1128/IAI.00349-15.
48. Elias, A.F., Stewart, P.E., Grimm, D., Caimano, M.J., Eggers, C.H., Tilly, K., Bono, J.L., Akins, D.R., Radolf, J.D., Schwan, T.G., and Rosa, P. (2002). Clonal polymorphism of Borrelia burgdorferi strain B31 MI: implications for mutagenesis in an infectious strain background. Infect Immun *70*, 2139-2150. 10.1128/IAI.70.4.2139-2150.2002.
49. Wiedow, O., Harder, J., Bartels, J., Streit, V., and Christophers, E. (1998). Antileukoprotease in human skin: an antibiotic peptide constitutively produced by keratinocytes. Biochem Biophys Res Commun *248*, 904-909. 10.1006/bbrc.1998.9069.
50. Nishimura, J., Saiga, H., Sato, S., Okuyama, M., Kayama, H., Kuwata, H., Matsumoto, S., Nishida, T., Sawa, Y., and Akira, S. (2008). Potent antimycobacterial activity of mouse secretory leukocyte protease inhibitor. The Journal of Immunology *180*, 4032-4039.
51. Hiemstra, P.S., Maassen, R.J., Stolk, J., Heinzel-Wieland, R., Steffens, G.J., and Dijkman, J.H. (1996). Antibacterial activity of antileukoprotease. Infect Immun *64*, 4520-4524. 10.1128/iai.64.11.4520-4524.1996.

844 52. Ramamoorthi, N., Narasimhan, S., Pal, U., Bao, F., Yang, X.F., Fish, D., Anguita,
845 J., Norgard, M.V., Kantor, F.S., Anderson, J.F., et al. (2005). The Lyme disease
846 agent exploits a tick protein to infect the mammalian host. Nature *436*, 573-577.
847 10.1038/nature03812.
848 53. Schuijt, T.J., Hovius, J.W., van Burgel, N.D., Ramamoorthi, N., Fikrig, E., and van
849 Dam, A.P. (2008). The tick salivary protein Salp15 inhibits the killing of serum-
850 sensitive Borrelia burgdorferi sensu lato isolates. Infect Immun *76*, 2888-2894.
851 10.1128/IAI.00232-08.
852 54. Crandall, H., Dunn, D.M., Ma, Y., Wooten, R.M., Zachary, J.F., Weis, J.H., Weiss,
853 R.B., and Weis, J.J. (2006). Gene expression profiling reveals unique pathways
854 associated with differential severity of lyme arthritis. J Immunol *177*, 7930-7942.
855 10.4049/jimmunol.177.11.7930.
856 55. Nugteren, S., and Samsom, J.N. (2021). Secretory Leukocyte Protease Inhibitor
857 (SLPI) in mucosal tissues: Protects against inflammation, but promotes cancer.
858 Cytokine & Growth Factor Reviews *59*, 22-35.
859 56. Lochhead, R.B., Strle, K., Kim, N.D., Kohler, M.J., Arvikar, S.L., Aversa, J.M., and
860 Steere, A.C. (2017). MicroRNA Expression Shows Inflammatory Dysregulation
861 and Tumor-Like Proliferative Responses in Joints of Patients With Postinfectious
862 Lyme Arthritis. Arthritis Rheumatol *69*, 1100-1110. 10.1002/art.40039.
863 57. Grillon, A., Scherlinger, M., Boyer, P.H., De Martino, S., Perdriger, A., Blasquez,
864 A., Wipff, J., Korganow, A.S., Bonnard, C., Cantagrel, A., et al. (2019).
865 Characteristics and clinical outcomes after treatment of a national cohort of PCR-
866 positive Lyme arthritis. Semin Arthritis Rheum *48*, 1105-1112.
867 10.1016/j.semarthrit.2018.09.007.
868 58. Deshmane, S.L., Kremlev, S., Amini, S., and Sawaya, B.E. (2009). Monocyte
869 chemoattractant protein-1 (MCP-1): an overview. J Interferon Cytokine Res *29*,
870 313-326. 10.1089/jir.2008.0027.
871 59. Lally, F., Smith, E., Filer, A., Stone, M.A., Shaw, J.S., Nash, G.B., Buckley, C.D.,
872 and Rainger, G.E. (2005). A novel mechanism of neutrophil recruitment in a
873 coculture model of the rheumatoid synovium. Arthritis Rheum *52*, 3460-3469.
874 10.1002/art.21394.
875 60. Grillet, B., Pereira, R.V.S., Van Damme, J., Abu El-Asrar, A., Proost, P., and
876 Opdenakker, G. (2023). Matrix metalloproteinases in arthritis: towards precision
877 medicine. Nat Rev Rheumatol *19*, 363-377. 10.1038/s41584-023-00966-w.
878 61. Chang, Y.H., Lin, I.L., Tsay, G.J., Yang, S.C., Yang, T.P., Ho, K.T., Hsu, T.C., and
879 Shiau, M.Y. (2008). Elevated circulatory MMP-2 and MMP-9 levels and activities
880 in patients with rheumatoid arthritis and systemic lupus erythematosus. Clin
881 Biochem *41*, 955-959. 10.1016/j.clinbiochem.2008.04.012.
882 62. Wen, G., Zhang, C., Chen, Q., Luong, I.A., Mustafa, A., Ye, S., and Xiao, Q.
883 (2015). A Novel Role of Matrix Metalloproteinase-8 in Macrophage Differentiation
884 and Polarization. J Biol Chem *290*, 19158-19172. 10.1074/jbc.M114.634022.
885 63. Lin, B., Kidder, J.M., Noring, R., Steere, A.C., Klempner, M.S., and Hu, L.T.
886 (2001). Differences in synovial fluid levels of matrix metalloproteinases suggest
887 separate mechanisms of pathogenesis in Lyme arthritis before and after antibiotic
888 treatment. J Infect Dis *184*, 174-180. 10.1086/322000.

64. Behera, A.K., Hildebrand, E., Scagliotti, J., Steere, A.C., and Hu, L.T. (2005). Induction of host matrix metalloproteinases by Borrelia burgdorferi differs in human and murine lyme arthritis. Infect Immun *73*, 126-134. 10.1128/IAI.73.1.126-134.2005.
65. Tarhini, M.F.H., Bentaher, A., Greige-Gerges, H., and Elaissari, A. (2018). A potential new strategy for using elastase and its inhibitor as therapeutic agents. J. Transl. Sci *5*, 1-8.
66. Takayama, K., Rothenberg, R.J., and Barbour, A.G. (1987). Absence of lipopolysaccharide in the Lyme disease spirochete, Borrelia burgdorferi. Infect Immun *55*, 2311-2313. 10.1128/iai.55.9.2311-2313.1987.
67. Bernard, Q., Smith, A.A., Yang, X., Koci, J., Foor, S.D., Cramer, S.D., Zhuang, X., Dwyer, J.E., Lin, Y.P., Mongodin, E.F., et al. (2018). Plasticity in early immune evasion strategies of a bacterial pathogen. Proc Natl Acad Sci U S A *115*, E3788-E3797. 10.1073/pnas.1718595115.
68. Matsuba, S., Yabe-Wada, T., Takeda, K., Sato, T., Suyama, M., Takai, T., Kikuchi, T., Nukiwa, T., and Nakamura, A. (2017). Identification of Secretory Leukoprotease Inhibitor As an Endogenous Negative Regulator in Allergic Effector Cells. Front Immunol *8*, 1538. 10.3389/fimmu.2017.01538.
69. Nakamura, A., Mori, Y., Hagiwara, K., Suzuki, T., Sakakibara, T., Kikuchi, T., Igarashi, T., Ebina, M., Abe, T., and Miyazaki, J. (2003). Increased susceptibility to LPS-induced endotoxin shock in secretory leukoprotease inhibitor (SLPI)-deficient mice. The Journal of experimental medicine *197*, 669-674.
70. Wilson, T., Kaur, N., Davis, J., and Ali, S.A. (2021). Tissue Collection and RNA Extraction from the Human Osteoarthritic Knee Joint. J Vis Exp. 10.3791/62718.
71. Zheng, H., and McAlinden, A. (2021). RNA Isolation from Articular Cartilage Tissue. Methods Mol Biol *2245*, 121-133. 10.1007/978-1-0716-1119-7_9.
72. Maffia, P.C., Zittermann, S.E., Scimone, M.L., Tateosian, N., Amiano, N., Guerrieri, D., Lutzky, V., Rosso, D., Romeo, H.E., Garcia, V.E., et al. (2007). Neutrophil elastase converts human immature dendritic cells into transforming growth factor-beta1-secreting cells and reduces allostimulatory ability. Am J Pathol *171*, 928-937. 10.2353/ajpath.2007.061043.
73. Schwendinger, M.G., O'Rourke, M., Traweger, A., Savidis-Dacho, H., Pilz, A., Portsmouth, D., Livey, I., Barrett, P.N., and Crowe, B.A. (2013). Evaluation of OspA vaccination-induced serological correlates of protection against Lyme borreliosis in a mouse model. PLoS One *8*, e79022. 10.1371/journal.pone.0079022.